Adenosine uptake is the major effector of extracellular ATP toxicity in human cervical cancer cells

Paola de Andrade Mello[a], Eduardo Cremonese Filippi-Chiela[b], Jéssica Nascimento[a], Aline Beckenkamp[a], Danielle Bertodo Santana[a], Franciele Kipper[b], Emerson André Casali[c], Alessandra Nejar Bruno[d], Juliano Domiraci Paccez[e], Luiz Fernando Zerbini[e], Marcia Rosângela Wink[f], Guido Lenz[b], and Andréia Buffon[a]

[a]Laboratory of Biochemical and Cytological Analysis, Faculty of Pharmacy, Federal University of Rio Grande do Sul, Porto Alegre, RS 90610-000, Brazil; [b]Department of Biophysics and Center of Biotechnology, Federal University of Rio Grande do Sul, Porto Alegre, RS 91501-970, Brazil; [c]Department of Morphological Science and Department of Biochemistry, Institute of Health Sciences, Federal University of Rio Grande do Sul, Porto Alegre, RS 90000-000, Brazil; [d]Federal Institute of Education, Science and Technology, Porto Alegre, RS 90035-007, Brazil; [e]International Center for Genetic Engineering and Biotechnology, Cancer Genomics Group, Cape Town 7925, South Africa; [f]Laboratory of Cell Biology, Federal University of Health Sciences of Porto Alegre, Porto Alegre, RS 90050-170, Brazil

ABSTRACT **In cervical cancer, HPV infection and disruption of mechanisms involving cell growth, differentiation, and apoptosis are strictly linked with tumor progression and invasion. Tumor microenvironment is ATP and adenosine rich, suggesting a role for purinergic signaling in cancer cell growth and death. Here we investigate the effect of extracellular ATP on human cervical cancer cells. We find that extracellular ATP itself has a small cytotoxic effect, whereas adenosine formed from ATP degradation by ectonucleotidases is the main factor responsible for apoptosis induction. The level of P2×7 receptor seemed to define the main cytotoxic mechanism triggered by ATP, since ATP itself eliminated a small subpopulation of cells that express high P2×7 levels, probably through its activation. Corroborating these data, blockage or knockdown of P2×7 only slightly reduced ATP cytotoxicity. On the other hand, cell viability was almost totally recovered with dipyridamole, an adenosine transporter inhibitor. Moreover, ATP-induced apoptosis and signaling—p53 increase, AMPK activation, and PARP cleavage—as well as autophagy induction were also inhibited by dipyridamole. In addition, inhibition of adenosine conversion into AMP also blocked cell death, indicating that metabolization of intracellular adenosine originating from extracellular ATP is responsible for the main effects of the latter in human cervical cancer cells.**

Monitoring Editor
Carl-Henrik Heldin
Ludwig Institute for Cancer Research

Received: Feb 6, 2014
Revised: Jun 23, 2014
Accepted: Jul 28, 2014

INTRODUCTION

Cervical cancer, although easily preventable by Papanicolaou screenings, is still high in the rank of cancers affecting women, with the third-highest incidence and fourth-highest fatality rate among females worldwide (Jemal *et al.*, 2011). Although almost all cases of cervical cancer are linked with human papillomavirus (HPV) infection, virus presence per se is not sufficient to trigger carcinogenesis. Acute infection with carcinogenic-type HPV is the first step, followed by viral persistence (rather than clearance) and subsequent precancer development and invasion (Schiffman *et al.*, 2011). This dynamic process suggests that alterations in growth and differentiation of epithelial cells are involved in cancer progression. Thus, understanding cervical cell biology and the mechanisms by which cells become altered during cancer development is extremely necessary.

Among the extracellular purines, ATP is a key extracellular signaling molecule and participates in several physiological processes, including immune response, neurotransmission, vascular tonus,

This article was published online ahead of print in MBoC in Press (http://www.molbiolcell.org/cgi/doi/10.1091/mbc.E14-01-0042) on August 7, 2014.

Address correspondence to: Andréia Buffon (andreia.buffon@ufrgs.br).

Abbreviations used: ATPγS, adenosine 5′-*O*-(3 thiotriphosphate); BzATP, 2′,3′-*O*(4-benzoylbenzoyl)ATP; DIP, dipyridamole; EGTA, ethylene-bis(oxyethylenenitrilo) tetraacetic acid; LDH, lactate dehydrogenase; oATP, oxidized ATP; zAsp, zAsp-CH2-DCB.

pain sensation, cell proliferation, differentiation, development, and death (Lee *et al.*, 2006; Tamajusuku *et al.*, 2010). To execute these functions, ATP can act through two types of purine receptors: P2X receptors, which are ligand-gated ion channels; and P2Y receptors, which are G protein–coupled receptors (Burnstock *et al.*, 2012).

Among the P2X receptors, only the P2×7 subtype is able to form a pore permeable to hydrophilic molecules up to 900 Da in size when activated by high ATP concentration over relatively long periods. This pore formation leads to an increase in intracellular cytosolic free calcium ions and the induction of cell death (Burnstock *et al.*, 2012). High levels of extracellular ATP and 2′,3′-*O*(4-benzoylbenzoyl)ATP (BzATP, a P2×7 receptor agonist) induce a significant reduction in keratinocyte number in primary human keratinocyte cultures, indicating the role of P2×7 in the control of epithelial growth (Burnstock *et al.*, 2012). In the same way, P2×7 was found to control baseline apoptosis in normal human ectocervical epithelial cells (hECEs) through an autocrine/paracrine mechanism involving ATP secretion by cells, P2×7 activation, cytosolic calcium influx, and mitochondrial apoptotic pathway induction (Wang *et al.*, 2004). Finally, Bian *et al.* (2013) described a role for P2×7 in ATP-induced autophagy in melanoma and colon cancer cells through the modulation of two important intracellular pathways involved in cell growth and death, phosphoinositide 3-kinase (PI3K)/Akt and AMP-activated protein kinase (AMPK)/PRAS40/mTOR. However, the role of autophagy in this context was not assessed.

Autophagy is a physiological mechanism involved in the degradation of old and/or injured cell components. It is triggered by metabolic alterations, such as nutrient deprivation or hypoxia, toxins, cytotoxic drugs, or other stressful conditions, and interferes with cell fate in a dual manner: it contributes to cell survival and adaptation in an adverse context but can contribute to cell death if triggered in high levels or for a long time (He and Klionsky, 2009; Yang and Klionsky, 2010). Two important components in this process are the proteins LC3 and p62. LC3 (microtubule-associated protein 1 light chain 3 α) is cytosolic (LC3 I) and, after proautophagic stimulus, is lipidated to form LC3 II (Kabeya *et al.*, 2004). P62 (sequestosome 1), on the other hand, marks cell components to be targeted to autophagosomal degradation and directly interacts with LC3 II in the autophagosomal membrane, being reduced when autophagic flux is increased (Pankiv *et al.*, 2007; Matsumoto *et al.*, 2011).

In addition to the direct cytotoxic effect described by extracellular ATP through P2×7 activation, other adenine nucleotides and adenosine can act as cell death inducers. Among them, adenosine, historically recognized as a key modulator of tumor progression, has emerged as an important factor in cell death and differentiation (Saitoh *et al.*, 2004; Sai *et al.*, 2006). Extracellular adenosine at high concentration can induce apoptosis in a variety of cancer cells via an intrinsic and/or an extrinsic pathway. The former pathway was described in human epithelial cancer cells originating from breast, colon, and ovary and is marked by adenosine uptake into cells via specific transporters, conversion to AMP by adenosine kinase, and AMPK activation (Saitoh *et al.*, 2004). The latter pathway was found in glioma cells, myeloid leukemia cells, mammary carcinoma cells, embryonic epithelial cells, granulose cells, thymocytes, and B lymphocytes and neutrophils and is characterized by adenosine as activation of the A_1, A_{2a}, A_{2b}, and A_3 receptors (Saitoh *et al.*, 2004; Sai *et al.*, 2006; Tsuchiya *et al.*, 2012). Depending on cell type, intracellular adenosine can induce apoptosis by a caspase-dependent or -independent mechanism (Tsuchiya *et al.*, 2012).

Tumor microenvironment is rich in extracellular ATP (Pellegatti *et al.*, 2008) and adenosine (Ohta *et al.*, 2006; Ghiringhelli *et al.*, 2012), and the effect of these molecules depends on both ATP concentration and the rate of ATP degradation to adenosine by ectonucleotidases present at the extracellular membrane (Beckenkamp *et al.*, 2014), as well as on the panel of P2 receptor expressed by the tumor (Di Virgilio, 2012; Burnstock and Di Virgilio, 2013). Therefore, to understand this complex network in the context of cancer development, here we studied the effect of extracellular ATP and its metabolite adenosine on cervical cancer cells. Therefore we investigated the importance of P2×7 and the mechanism underling ATP toxicity on cervical cancer, searching for a possible new target for diagnosis, prognosis, or treatment of this neoplasia.

RESULTS

SiHa cell line expresses high mRNA levels of the P2×7 receptor

Because lower levels of P2×7 were described in epithelial cancer cells than in normal tissue (Li *et al.*, 2009), we investigated the levels of P2×7 mRNA in different cervical cancer cell lines and in an immortalized human epithelial cell line (HaCaT) used as nontumorigenic control cells (Figure 1A). Cervical cancer cell lines (SiHa, HeLa, and C33A) and HaCaT exhibited different amounts of P2×7 mRNA. Among them, the SiHa cell line presented the highest levels of P2×7 mRNA, and therefore we chose it to investigate the role of P2×7 in the response of cervical cancer to extracellular ATP.

Extracellular ATP promotes cell death in a dose- and time-dependent way

To initially assess the cytotoxic effect of extracellular ATP, we treated cervical cancer cells with increasing doses of ATP for 24 h, with a maximum cytotoxic effect of 30% with 5 mM (Figure 1B). After 72 h, 5 mM ATP reduced the number of cells by 80% in relation to control (Figure 1C, bottom). Surviving cells had reduced long-term viability, since clonogenic survival of cells that survived 72 h was only 31%, indicating a slow mechanism of cell death (Figure 1C, top).

Extracellular ATP–induced cell death shows features of apoptosis but not necrosis

ATP, 5 mM, led to cell shrinkage in a time-dependent manner, as observed by forward scatter, suggesting apoptotic cell death (Figures 2A and Supplemental Figure S1). Indeed, treatment with extracellular ATP induced only a slight increase of lactate dehydrogenase (LDH) levels in the culture medium after 72 h (Figure 2B) and no increase of propidium iodide (PI) staining (Figure 2C), showing that necrosis was not the primary mechanism of ATP toxicity in SiHa cells. On the other hand, cells presented some phenotypic alterations that resemble apoptosis, including membrane blebbing, cell shrinkage, and chromatin condensation after 48 and 72 h. In agreement, ATP treatment highly increased annexin V staining (Figure 2C), confirming that ATP exerts a cytotoxic effect in SiHa cancer cells mainly through induction of apoptotic cell death.

ATP-induced apoptosis is not prevented by caspases inhibitors or calcium chelators

The main mechanism of P2×7-mediated cell death in normal human ectocervical epithelial cells (hECEs) involves pore formation, calcium influx, and apoptosis induction through caspase activation (Wang *et al.*, 2004). Surprisingly, neither ethylene-bis(oxyethylenenitrilo) tetraacetic acid (EGTA) nor the pancaspase inhibitor zAsp-CH(2)-DCB (zAsp) was able to reduced ATP toxicity (Figure 3A). Of interest, BzATP, a P2×7 agonist, showed a cytotoxic effect in a dose-dependent manner, with $EC_{50} \approx 100$ μM (Figure 3B), and this cytotoxicity was apoptotic and completely blocked by EGTA and zAsp (Figure 3A), suggesting that P2×7 is functional in inducing cell death but

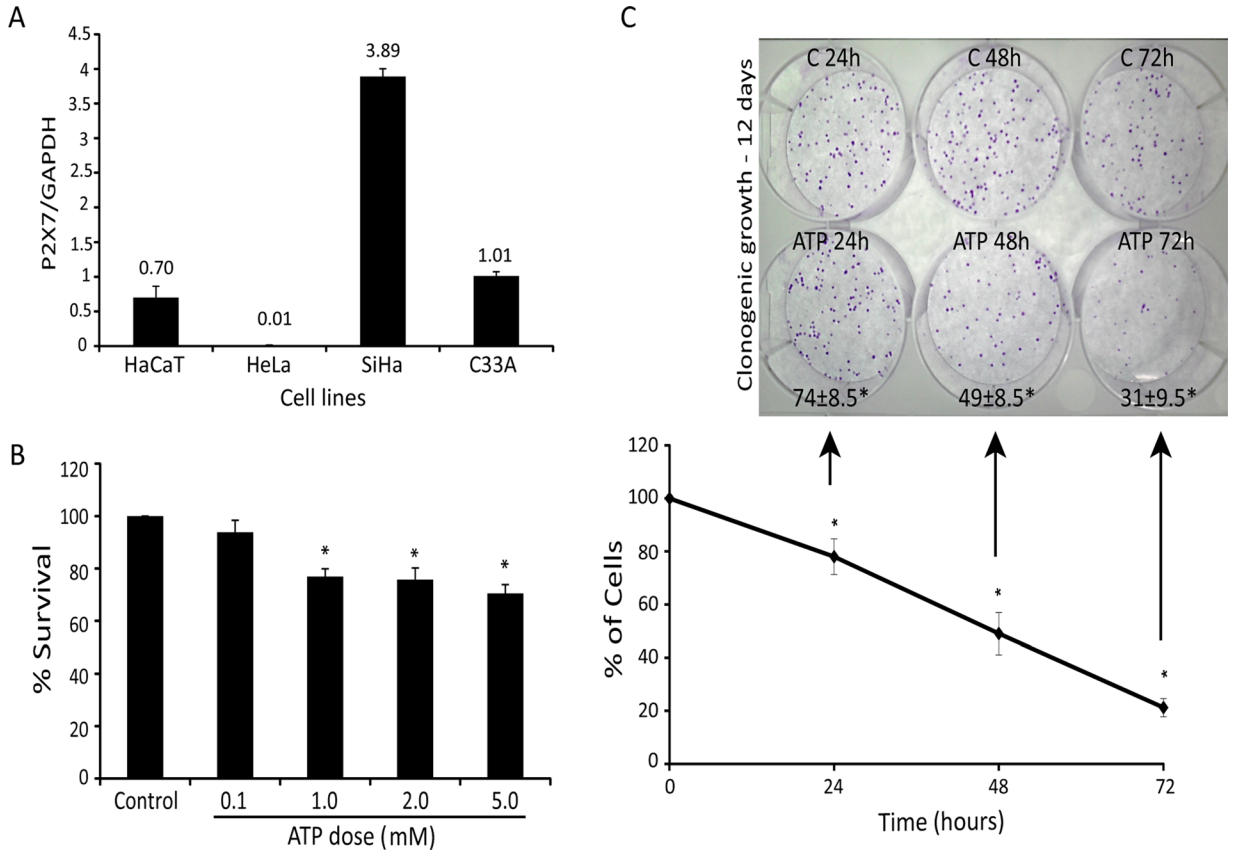

FIGURE 1: Extracellular ATP exerts acute and chronic toxicity in cervical cancer cells. (A) Comparison of P2×7 mRNA expression in SiHa, HeLa, C33A, and HaCaT cell lines by quantitative real-time PCR analysis. Results are presented as the ratio cDNA/GAPDH. (B) SiHa cell viability after exposure to increased ATP concentration for 24 h using MTT assay. (C) Bottom, time curve of SiHa cells treated with 5 mM ATP for 24, 48, and 72 h, determined by number of viable cells not marked by trypan blue. Top, 100 viable cells were seeded in clonogenic assay, and colony formation was evaluated. Numbers at bottom are survival fraction according to clonogenic assay. C, control; ATP, treatment with 5mM ATP. *$p < 0.05$ compared with control (one-way ANOVA, followed by Tukey's test).

does not respond to concentrations of ATP above the described concentration needed for activation of this receptor. In addition, when SiHa cells were treated with ATPγS, a nondegradable ATP form, only ~20% of cells died (Figure 3C), which was completely blocked by calcium chelation and caspase inhibition (Figure 3, C and D), indicating that a degradation product of ATP plays a role in its cytotoxicity.

This relatively small contribution of P2×7 to cell death was confirmed with the use of a P2×7 antagonist, oxidized ATP (oATP), which only partially prevented the effect of ATP (Figure 4A). To reinforce these findings, P2×7 knockdown (KD) SiHa cells (Figure 4B) were slightly more resistant to ATP than were wild-type (WT) or KD control cells (Figure 4C), confirming the partial role of this receptor in the cytotoxic effect of ATP.

ATP treatment preferentially eliminates cells expressing high P2×7 levels

To investigate which cells are killed by ATP directly, we determined the P2×7 protein levels in cells after treatment with ATP in two ways: 1) cells were treated with 5 mM ATP for 24, 48, and 72 h, and the remaining adherent cells were lysed and tested for P2×7 levels (Figure 5A); and 2) cells were treated with 5 mM ATP for 24, 48, and 72 h, followed by medium removal, two washes with 1× phosphate-buffered saline (PBS), and growth in ATP-free medium for an additional 4 d; adherent cells were then collected, and Western blot analysis was performed (Figure 5B). As shown in Figure 5, A and B, in both treatments, cells that remained adherent showed lower P2×7 protein levels than control, indicating that a subpopulation of cells with higher P2×7 levels was eliminated by ATP, as was also observed in glioma cells (Tamajusuku *et al.*, 2010). Together these results suggest that extracellular ATP per se is responsible for only a small part (~20%) of the toxicity of extracellular ATP through the P2×7 receptor and that the remaining cytotoxic effect might be through a metabolite derivative.

Adenosine uptake formed from ATP degradation is the major cytotoxic factor of extracellular ATP

Thus far our data suggest that P2×7 activation per se only eliminates cells with high expression levels of P2×7. To understand where the additional toxicity of ATP comes from, we turned our attention to adenine nucleotides and adenosine formed from ATP by the action of ectonucleotidases, which are expressed in human cervical cancer cells (Beckenkamp *et al.*, 2014). Most of the extracellular ATP was degraded to its metabolites over 72 h (Figure 6A; see also Supplemental Table S1). All of the main metabolites of ATP had toxic effects in cervical cancer cell lines (SiHa, HeLa, and C33A) and a human epithelial cell line (HaCaT), with C33A and HeLa cells presenting a more resistant profile. Of importance, only adenosine significantly reduced cell viability in all cell lines (Figures 6B and Supplemental Figure S3A). Because several studies

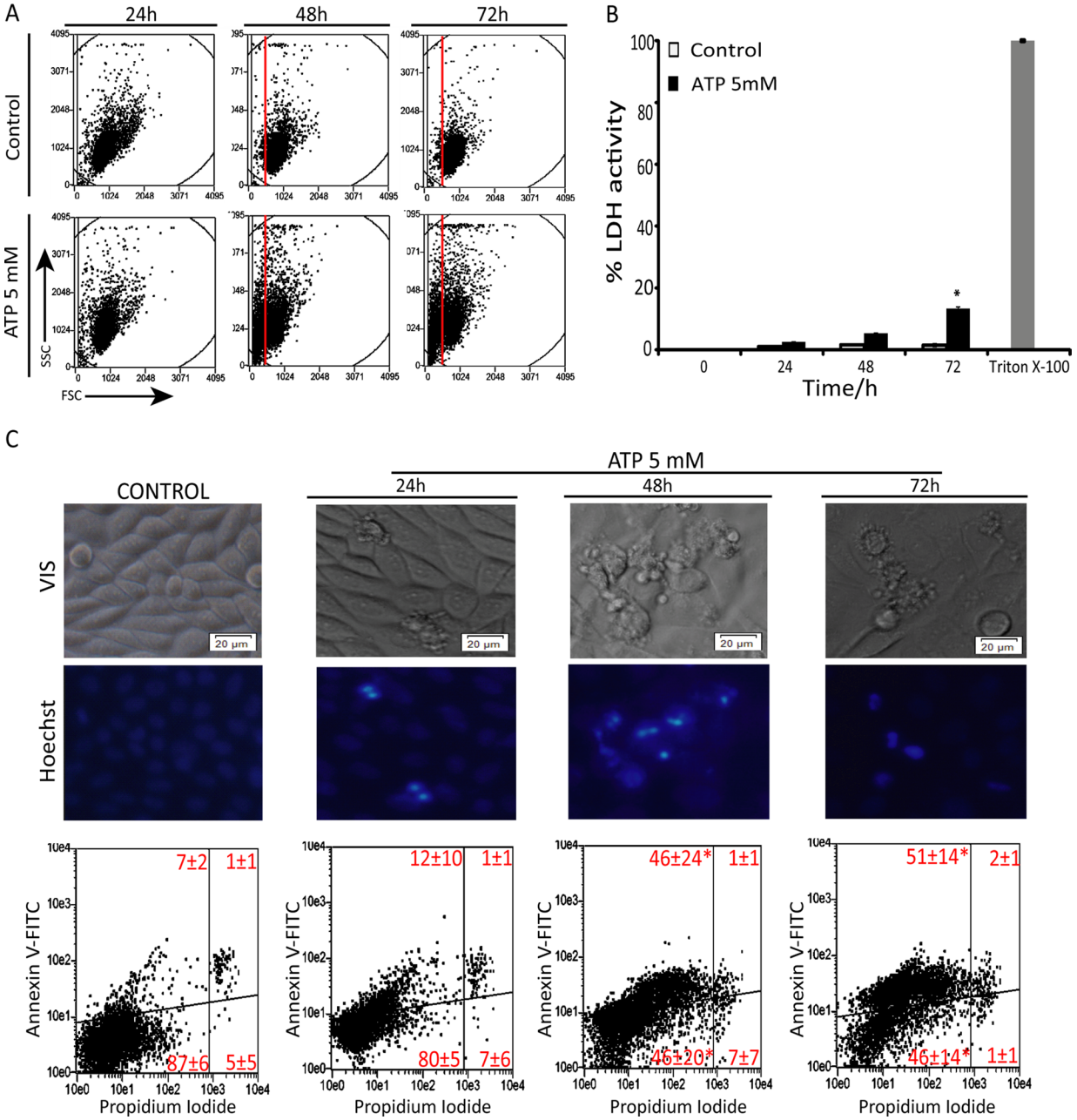

FIGURE 2: Extracellular ATP triggers apoptosis in SiHa cervical cancer cells. (A) Forward scatter analysis after treatment with 5 mM ATP for 24, 48, and 72 h. (B) Loss of membrane integrity measured by LDH release after treatment with 5 mM ATP for 24, 48 and 72 h. Triton X-100 was used as positive control for LDH release. (C) Top, images of SiHa cell treatment with 5 mM ATP for 24, 48, and 72 h. Cell nuclei was stained with Hoescht 35565665 according to manufacturer's instruction. Note apoptotic features such as cell shrinkage and blebbing and fragmented nuclei when cells were treated with ATP. Scale bars, 20 μm; magnification, 20×. Bottom, apoptosis and necrosis measured by annexin V– and PI-positive cells, quantified by flow cytometry in the same conditions as in C. Values refer to average of the percentage of cells in each gate of three independent experiments ± SD. *$p < 0.05$ compared with control (one-way ANOVA, followed by Tukey's test).

attributed a cytotoxic effect to adenosine in other cell types (Saitoh *et al.*, 2004; Sai *et al.*, 2006), we investigated whether uptake of extracellular adenosine formed by ATP degradation, which did not accumulate in extracellular medium (Supplemental Figure S5A), was responsible for apoptosis induction after ATP treatment. We treated SiHa cells with 10 μM dipyridamole (DIP), an inhibitor of adenosine transport, 30 min before ATP exposure (Figure 6C, left). DIP reduced cell shrinkage (Supplemental Figure S1), cell number reduction (Figure 6C, right), and annexin V staining (Figures 6D, right, and Supplemental Figure S1) induced by ATP treatment. Furthermore, phenotypic observation confirmed the reduction of apoptotic features such as cell shrinkage, membrane blebbing, and nuclear condensation and fragmentation (Figure 6D, left and middle), which were present after ATP treatment only (Figure 2C). After 72 h, there was a reduction of 20% in the cell number in DIP plus ATP treatment, which was not altered by DIP replacement each 24 h (unpublished data) but was by knockdown of the P2×7 receptor (Supplemental Figure S2), suggesting that

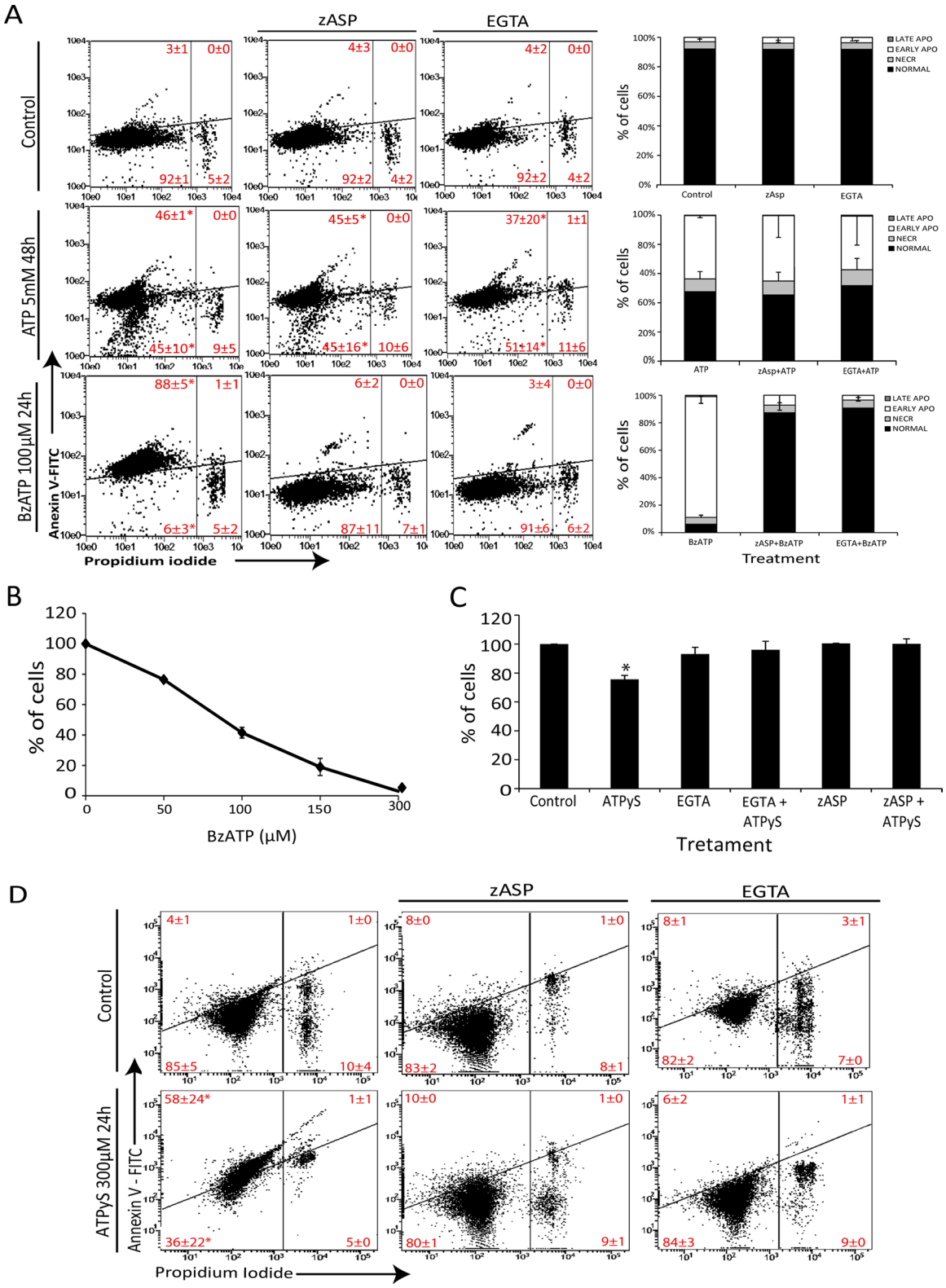

FIGURE 3: Extracellular ATP triggers apoptosis in a caspase- and calcium influx–independent way. (A) SiHa was exposed or not for 30 min to 0.6 mM EGTA or 50 µM zAsp, and then 5 mM ATP or 100 µM BzATP was added for 48 or 24 h, respectively, and apoptosis and necrosis was measured according to annexin V/PI binding (see *Materials and Methods*). Right, average values measured in each gate. NORMAL cells, annexin V–/IP–; NECR cells annexin, V–/IP+; EARLY APO cells, annexin V+/IP–; LATE APO cells, annexin V+/IP+. (B) Dose–response curve of BzATP treatment for 24 h measured with number of viable cells using trypan blue dye exclusion. (C) Number of viable cells not stained with trypan blue, after exposure of SiHa cells to 300 µM nondegradable ATP, ATPγS, for 24 h with or without previous exposure to 0.6 mM EGTA or 50 µM zAsp. (D) Apoptosis and necrosis induction at these same conditions. *$p < 0.05$ compared with other treatments (two-way ANOVA, followed by Bonferroni posttest).

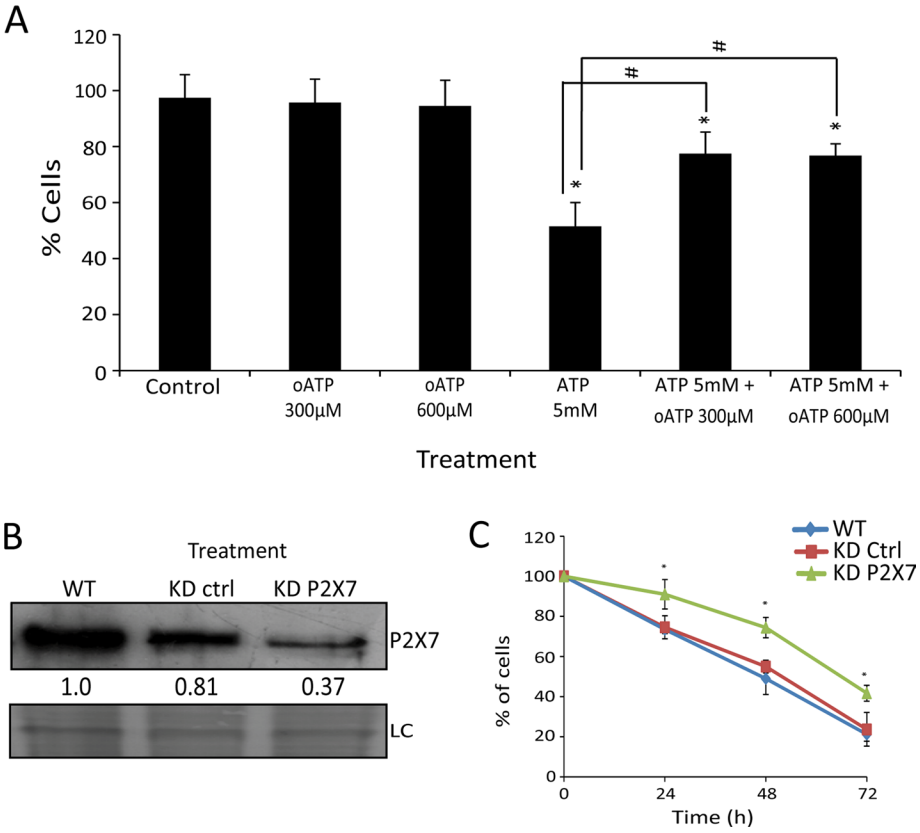

FIGURE 4: P2×7 receptor contributes little to the total cytotoxic effect of extracellular ATP in SiHa cells. (A) Blockage of 5 mM ATP induces cell death by the P2×7 antagonist oATP at two concentrations (300 and 600 µM). Control represents cells without treatment. *$p < 0.05$ for comparison vs. control and #$p < 0.05$ for comparison vs. respective group (two-way ANOVA, followed by Bonferroni posttest). (B) Knockdown for P2×7 confirmed by Western blot. SiHa WT, SiHa wild type; SiHa KD ctrl, SiHa cells transduced with nontarget sequence (knockdown control); SiHa KD P2×7, SiHa knockdown for P2×7. Loading control (LC) represents PVDF membrane stained with Coomassie blue. Numbers represent P2×7 protein amount in relation to SiHa WT. (C) Number of viable cells not marked by trypan blue after 5 mM ATP treatment for 24, 48, and 72 h. *$p < 0.05$ vs. SiHa KD Ctrl and WT at the respective times (one-way ANOVA, followed by Tukey's test).

this slight effect occurs through ATP-mediated P2×7 receptor activation and toxicity and is not due to the loss of action of DIP. Taken together, these results strongly suggest that adenosine uptake, formed by ATP degradation, is a central player in the cell death induced by extracellular ATP. In agreement, inhibition of adenosine kinase by ABT-702 completely reversed ATP-induced apoptosis (Figure 6E, bottom), indicating that intracellular adenosine phosphorylation and conversion to AMP is a key step in the toxicity of extracellular ATP. Indeed, as occurred with DIP plus ATP, there was a reduction of 20% in the number of cells after 72 h of treatment with ABT-702 plus ATP (Figure 6E, top), reinforcing the slight involvement of ATP-P2×7 in ATP-induced cell death and the importance of the metabolization of adenosine to AMP. Corroborating these data, sensitivity of cells to adenosine was strongly positively correlated ($r = 0.9$) with ATP cytotoxic effect in the four cell lines studied. On the other hand, ATP sensitivity at 24 h was not correlated with mRNA P2×7 levels (Supplemental Figure S3). Of interest, when cells were exposed to ATP for 48 or 72 h, the correlation between ATP sensitivity and mRNA P2×7 levels increased (unpublished data), suggesting that P2×7 activation could be important after a long exposure and thus could be involved with the cell death observed after DIP plus ATP at 72 h.

Adenosine uptake promotes dATP accumulation and intracellular nucleotide/nucleoside level imbalance, activates AMPK, increases p53, and induces autophagy

Measurement of intracellular nucleotides/nucleosides, as well as of deoxy-ATP (dATP), after ATP exposure pointed to an imbalance in the pool of nucleotides/nucleosides and an accumulation of dATP. Moreover, all of these intracellular effects were completely blocked by DIP (Supplemental Figure S5, B and C), suggesting that adenosine uptake alters the balance of intracellular nucleotide/nucleoside levels.

Extracellular ATP increased the levels of pAMPK(T172)—the active state of AMPK (Hardie *et al.*, 2006)—in a time-dependent manner, mainly after 48 and 72 h, accompanied by PARP cleavage (Figure 7A). p53 levels reached the highest levels at 48 h and these molecular alterations were suppressed almost completely by DIP pretreatment. Furthermore, DIP pretreatment increased the levels of Bcl2, a classical antiapoptotic protein, after 72 h of ATP treatment. Taken together, these data suggest that adenosine uptake is responsible for the main molecular alterations that underlie the toxicity of extracellular ATP in cervical cancer cells.

The induction of autophagy by extracellular ATP has been described (Bian *et al.*, 2013), but the role of autophagy in this context is poorly understood, despite its importance. Thus we examined the induction of autophagy after ATP treatment, with or without DIP, as well as the role of ATP-induced autophagy. As shown in Figure 7B, 5 mM ATP increased the LC3II/I ratio and decreased the amount of p62 after 48 and 72 h, suggesting autophagy induction. Corroborating data from molecular mechanisms triggered by ATP treatment, this proautophagic effect of ATP was reverted by DIP pretreatment, suggesting that adenosine uptake is responsible for autophagy triggering after ATP treatment.

Finally, the role of ATP-induced autophagy was assessed by pharmacological modulation of this process, followed by cell number evaluation and acridine orange (AO) staining, which is a marker of autophagolysosome formation. ATP alone significantly increased the percentage of AO-positive cells after 24 h. To inhibit autophagy, cells were pretreated with two autophagy inhibitors, 3-methyladenine (3MA) and bafilomycin A1 (Baf), whereas autophagy was activated by rapamycin (RAPA). 3MA and Baf inhibited ATP-induced autophagy only until 24 h, whereas RAPA potentiated the proautophagic effect of ATP for up to 48 h (Figure 7, C and D, and Supplemental Figure S4). After 24 h, the treatments that increased in autophagy (Figure 7D, top) induced a reduction in cell number (Figure 7D, bottom), with strong correlation ($r = 0.9$) between autophagy and cell death (Supplemental Figure S4B), suggesting a cytotoxic role for ATP-induced autophagy. On the other hand, after 48 h, all treatments presented the same index of autophagy, and cell number in the presence of autophagy modulators reached a plateau (Figure 7D).

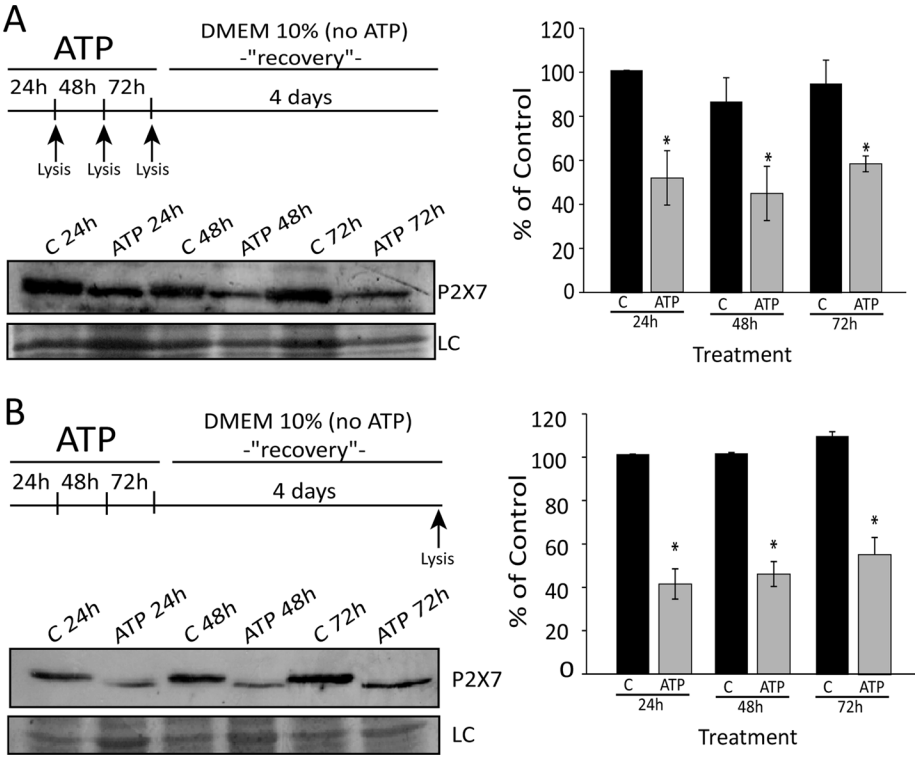

FIGURE 5: A subpopulation of cells with higher P2×7 levels was eliminated by ATP. (A) P2×7 protein expression analyzed by Western blot in SiHa cells that remain attached to the plate after treatment for 24, 48, and 72 h with 5 mM ATP and (B) after recovery with medium for 4 d. Note that expression of P2×7 is lower in an ATP-resistant subpopulation. C, control (no treatment); T, treatment with 5 mM ATP. *$p < 0.05$ vs. respective control (one-way ANOVA, followed by Tukey's test).

DISCUSSION

Among several receptors that comprise the purinergic system, the P2×7 subtype is implicated in terminal differentiation and apoptosis of stratified squamous epithelium and therefore has a special role in the control of cell death (Burnstock *et al.*, 2012). In human cervical epithelial cells, P2×7 activation by extracellular ATP culminates in pore opening, calcium influx, high cytosolic calcium, and apoptosis induction through the mitochondrial pathway (Wang *et al.*, 2004). When cervical cancer cells were exposed to high extracellular ATP, phenotypic features of apoptosis, such as cell shrinkage, membrane blebbing, and phosphatidylserine externalization, were found. However, in contrast to normal cervical epithelial cells, the induction of SiHa cell death by ATP, but not the nondegradable variants of ATP, did not occur by calcium influx and caspase activation. These data indicate that a caspase-independent mechanism could be involved in ATP-induced SiHa cell death. Recently Bian *et al.* (2013) described a new pathway for an antitumor effect of ATP on MCA38 colon cancer cells and on B16/F10 melanoma, which involves P2×7 activation and concurrent blockage of mTOR signaling through AMPK-PRAS40 and PI3K/AKT pathways, culminating in autophagy induction and cell death in a caspase- independent way. However, our data do not support such a major role for P2×7 in cervical cancer cell death. A pharmacological approach using oATP or P2×7silencing suppressed only 20% of the ATP-induced toxicity. Indeed, analyses of P2×7 levels in adherent cells that survived ATP cytotoxicity showed that only cells that expressed high levels of P2×7 were eliminated.

These data suggested that ATP could be acting also by producing a cytotoxic metabolite. Among ATP metabolites, extracellular adenosine exerted a cytotoxic effect in human epithelial cancer cells originating from breast, colon, and ovary. In these cells, adenosine leads to an increase in AMPK phosphorylation, probably through uptake and transformation into AMP by adenosine kinase, since this effect was blocked by the equilibrative nucleoside transporter (ENT) inhibitor dipyridamole (Saitoh *et al.*, 2004; Sai *et al.*, 2006). SiHa cell death was also marked by adenosine phosphorylation and transformation into AMP, which culminated in AMPK phosphorylation. In addition, p53 activation and PARP cleavage were also observed with ATP and blocked by DIP. In agreement with our results, treatment of human gastric cancer cells with adenosine-induced apoptosis independently of caspases and exclusively via an intrinsic pathway through AMPK activation (Saitoh *et al.*, 2004). In the same way, Nogi *et al.* (2012) found that AMP formed intracellularly from adenosine uptake induced an increase in p53 expression, resulting in malignant pleural mesothelioma cell death by caspase-independent apoptosis. Similar to our data, all of these effects were blocked by DIP, indicating that adenosine uptake was a key for apoptosis induction. Our work, however, also found a contribution of autophagy to SiHa cell death. This process seems to be important for ATP toxicity, since the increase of AO-positive cells strongly correlated with cell death after 24 h of treatment. However, the proautophagic effect of ATP was almost totally inhibited by DIP, indicating that this effect was mediated by adenosine uptake and not through P2×7 activation, as previously described in murine colon cancer cells and mouse melanoma cancer cells (Bian *et al.*, 2013).

Other evidence also suggests that adenosine is the main player responsible for ATP cytotoxicity, including the fact that extracellular AMP, which is not a ligand of any P2 receptors, also promotes cell death, indicating a role for adenosine formed from AMP degradation by 5 -nucleotidase on apoptosis induction (Wen and Knowles, 2003). Of importance, ATP and ADP can also be metabolized by ectonucleotidases at the cell surface of SiHa cells and generate adenosine (Beckenkamp *et al.*, 2014). Further evidence comes from our finding that after 72 h of treatment, DIP alone was able to inhibit ~80% of ATP-induced cell number reduction and block all ATP cytotoxicity in P2×7 KD cells. Additional evidence is provided by the fact that the adenosine metabolites inosine and hypoxanthine, although reaching high levels in extracellular medium and being transported into the cell by ENTs (Baldwin *et al.*, 2004), did not induce cell death, since preliminary data indicate a positive effect of inosine on proliferative but not cell death (unpublished data). Indeed, both inosine and hypoxanthine have been described as protective agents against cytotoxic compounds and hypoxic injury in normal and cancer cells (Obajimi and Melera, 2008; Ma *et al.*, 2011).

Increased intracellular levels of inosine and dATP after ATP exposure, which were blocked by DIP pretreatment, further support the entrance of adenosine into the cell. Accumulated dATP has been associated with accumulation of DNA strand breaks, activation of p53, and induction of apoptosis in lymphocytes (Joachims *et al.*, 2008; Johnston, 2011). Adenosine may promote cell death by

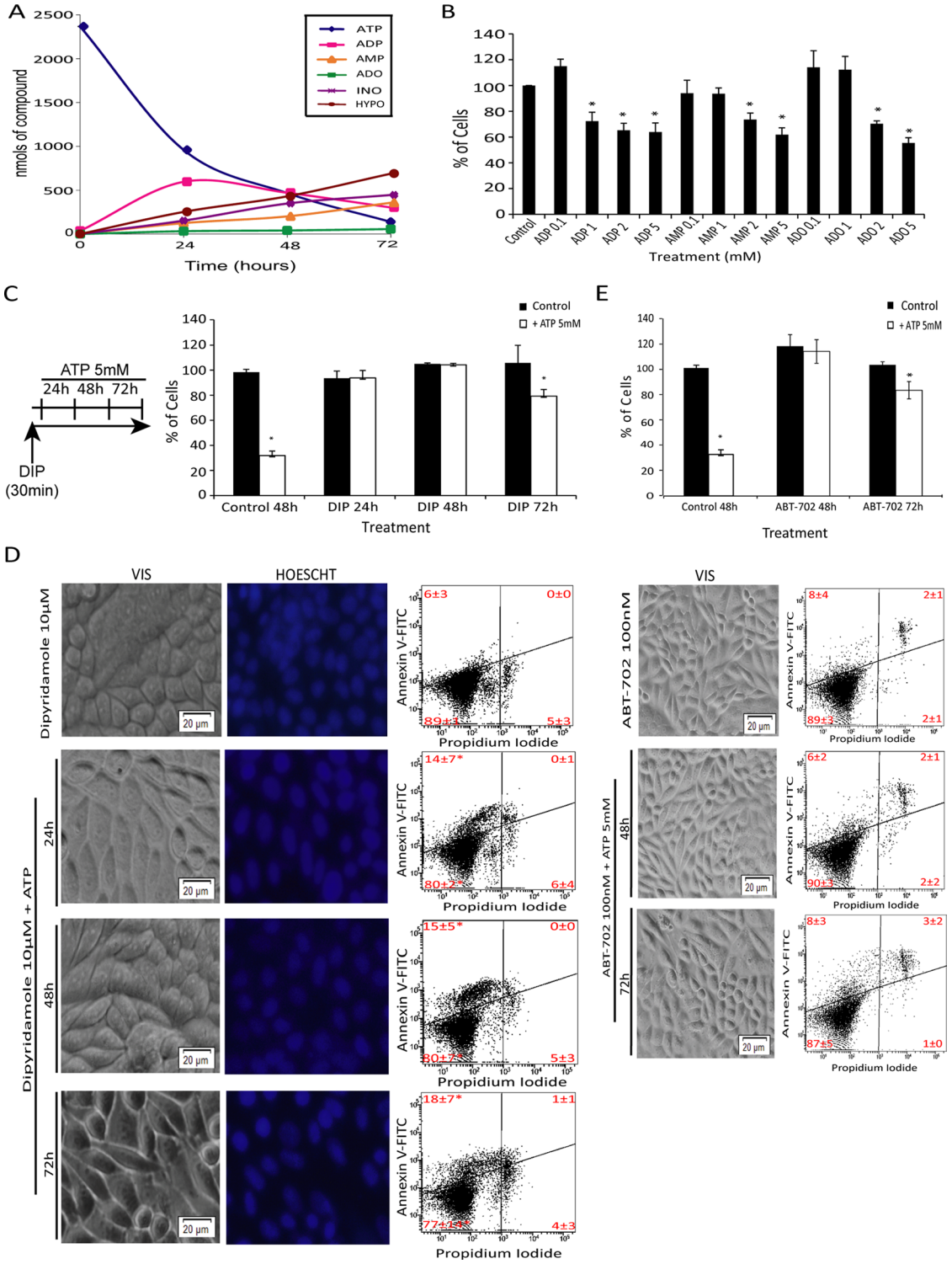

FIGURE 6: Adenosine uptake and conversion to AMP by adenosine kinase is the major mechanism of toxicity triggered by extracellular ATP in SiHa cells. (A) Extracellular ATP hydrolysis and product formation in SiHa cell line. Cells were incubated with 5 mM ATP, and levels of nucleotides in cell medium were analyzed by HPLC after treatment times of 0, 24, 48, and 72 h. A control without ATP was done for basal determination of nucleotides released by cells (Supplemental Table S1). ATP, ADP, AMP, adenosine (ADO), inosine (INO), and hypoxanthine (HYPO) contents in reaction medium were represented by exogenous (added) plus endogenous (secreted) purinergic compound as mean (nanomoles) ± SD. (B) Effect of ATP metabolites on SiHa cell death. Cells were incubated with different concentrations of ADP, AMP, and adenosine for 24 h, and the number of viable cells was determined as described in *Materials and Methods*. *$p < 0,05$ compared with control (one-way ANOVA, followed by Tukey's test). (C, D) Dipyridamole blockage of 5 mM ATP induces cell death by inhibiting extracellular adenosine uptake. SiHa cells were exposed to 10 µM dipyridamole alone or for 30 min, and then 5 mM ATP was added for 24, 48, and 72 h. (C) Number of viable cells after treatment. *$p < 0.05$ compared with control (two-way ANOVA, followed by Bonferroni posttest). (D) Apoptosis and necrosis index according

inducing an imbalance in deoxynucleotide triphosphate pools. Furthermore, we did not observe a correlation between P2×7 mRNA levels and ATP sensitivity, whereas adenosine and ATP sensitivity were highly correlated, indicating a preponderant role of the latter in relation to the former. Taken together, the evidence strongly suggests that adenosine formed from ATP metabolism, and not ATP itself, is the main agent responsible for SiHa cell death, contrary to what others found in other cell types (Wang *et al.*, 2004; Feng *et al.*, 2011; Di Virgilio, 2012; Bian *et al.*, 2013). Moreover, it seems that chronic exposure to micromolar levels of adenosine (100–200 µM) is a requirement for significant induction of cell death, in contrast to acute exposure, which requires millimolar levels. In both treatments, cells are exposed to a much higher concentration of adenosine than the amount found in the intracellular space (~10 nM; Kloor *et al.*, 2000). Wen and Knowles (2003) had already described a role for extracellular adenosine formed from ATP in a human hepatoma cell line death. However, in contrast to our result, they found that extracellular adenosine induced cell apoptosis via the A3 adenosine receptor. In our case, activation of the A3 receptor in cell death is unlikely, since DIP inhibited almost all cell death, and the SiHa cell line showed very low levels of A3 mRNA (unpublished data).

We propose that human cervical cancer cells comprise a heterogeneous population that responds differently to extracellular ATP toxicity according to the level of P2×7 receptor present in the cell membrane. Our hypothesis is that ATP per se is responsible for the elimination of a small subpopulation of cells (~20%) that express a high level of P2×7 and are killed through P2×7 activation, whereas adenosine acts in the remaining subpopulation, which is ATP resistant, expresses low levels of P2×7, and dies through adenosine uptake, AMPK phosphorylation, dATP accumulation, p53 activation, and autophagy induction (Figure 8). Thus cooperation among ATP and its metabolites seems to be important for cytotoxicity, with adenosine being necessary, but not sufficient, to induce cell death in the whole population of cells, which is of fundamental importance in cancer therapeutics. In conclusion, here we shed light on how cervical cancer cells respond to high extracellular ATP, which is a context commonly present in solid tumors and can be exploited to improve our understanding of tumor biology, as well as to increase therapy efficiency and overcome cell resistance.

MATERIALS AND METHODS

Reagents

Reagents, ATP, ADP, AMP, adenosine, BzATP, oATP, ATPγS, DIP, 3MA, BAF, RAPA, and AO were purchased from Sigma-Aldrich (St. Louis, MO). ABT-702, annexin V, and propidium iodide were purchased from Santa Cruz Biotechnology (Santa Cruz, CA). The pan caspase inhibitor zAsp-CH2-DCB (zAsp; Peptide Institute, Tokyo, Japan) was kindly provided by Fabiana Horn (UFRGS) and dissolved in dimethyl sulfoxide (DMSO; Acros Organics).

Cell culture

Three cervical carcinoma cell lines, SiHa, HeLa, and C33A (American Type Culture Collection, Rockville, MD), were used in this study. SiHa cells contain integrated HPV 16; HeLa cells carry integrated HPV 18; and C33A cells are HPV negative and contain mutant p53. All culture materials were purchased from Gibco Laboratories (Grand Island, NY). Cervical carcinoma cell lines were maintained in culture flask in low-glucose DMEM supplemented with 10% fetal bovine serum at 37°C in a 5% CO_2 atmosphere at 100% humidity. The spontaneously immortalized human epithelial cell line HaCaT was maintained at the same conditions but cultured with high-glucose DMEM.

Cell viability

Cell viability was assessed using the methylthiazolyltetrazolium bromide (MTT) assay. Cell lines (3500 cells/well) were seeded on 96-well multiwell plates, grown for 72 h, and treated with different concentration of ATP, ADP, AMP, and adenosine for 24 h at 37°C. After treatment, cells were incubated for 3 h at 37°C in MTT solution (0.5 mg/ml MTT dissolved in Ca^{2+}- and Mg^{2+}-free buffer). Formazan crystals formed by tetrazolium cleavage were dissolved with dimethyl sulfoxide (DMSO) and quantified at 570 and 630 nm using an EnVision Multilabel Plate Reader (PerkinElmer, Waltham, MA). Negative controls were made with DMEM supplemented with 10% fetal bovine serum (FBS). Results are expressed as percentage of control.

Cell counting

Cell lines (20,000 cells/well) were seeded on 24-well multiwell plates and treated with 5 mM ATP for 24, 48, and 72 h or with different concentrations of ADP, AMP, and adenosine for 24 h. At the end of treatment, the medium was removed, cells were washed with 1× PBS, and 200 µl of 0.25% trypsin/EDTA was added to detach the cells, which were counted in a hemocytometer (number of viable cells not marked by trypan blue). Negative controls were made with DMEM supplemented with 10% FBS. Results are expressed as percentage of control.

Clonogenic survival assays

Cells were assayed for the cytotoxic effect of ATP after cell survival according to established methods of performing the clonogenic assay (Franken *et al.*, 2006). Subconfluent cultures were exposed to 5 mM ATP for 24, 48, and 72 h. Then the surviving adherent cells were washed with PBS preheated to 37°C, trypsinized, counted, and replated in six-well plates (100 cells/well). After 12 d of incubation in complete culture medium, the colonies formed from each cell plated were stained with crystal violet after fixation with methanol and counted manually. In each case results are expressed as survival fraction, which was obtained by dividing the number of colonies that arise after treatment of cells by the number of cells seeded and plate efficiency (PE: number of colonies formed by untreated cells/number of cells seeded), multiplied by 100.

LDH activity measurement

Loss of membrane integrity was measured through LDH release. SiHa cells (20,000 cells/well) were seeded on 24-well multiwell plates and treated with 5 mM ATP for 24, 48, and 72 h. After cell medium

to annexin V/IP stain. Images were taken from SiHa cell line after the foregoing treatments. Cell nuclei were stained with Hoescht 35565665 according to manufacturer's instruction. Note the extinction of apoptotic features such as cell shrinkage and blebbing and fragmented nuclei when cells were treated with ATP only (Figure 2C). *$p < 0.05$ compared with dipyridamole alone (two-way ANOVA, followed by Bonferroni posttest). (E) Adenosine kinase inhibitor (ABT-702) blockage of 5 mM ATP induces cell death by inhibiting intracellularly transported adenosine phosphorylation and conversion to AMP. SiHa cells were exposed to 100 nM ABT-702 for 30 min and followed or not by 5 mM ATP for 48 and 72 h. ABT-702, 100 nM, was replaced each 24 h. Top, number of viable cells after treatment. *$p < 0.05$ compared with control (two-way ANOVA, followed by Bonferroni posttest). Bottom, apoptosis and necrosis index according to annexin V/IP stain and representative images of SiHa cells after foregoing treatments. Scale bars, 20 µm; magnification, 20×.

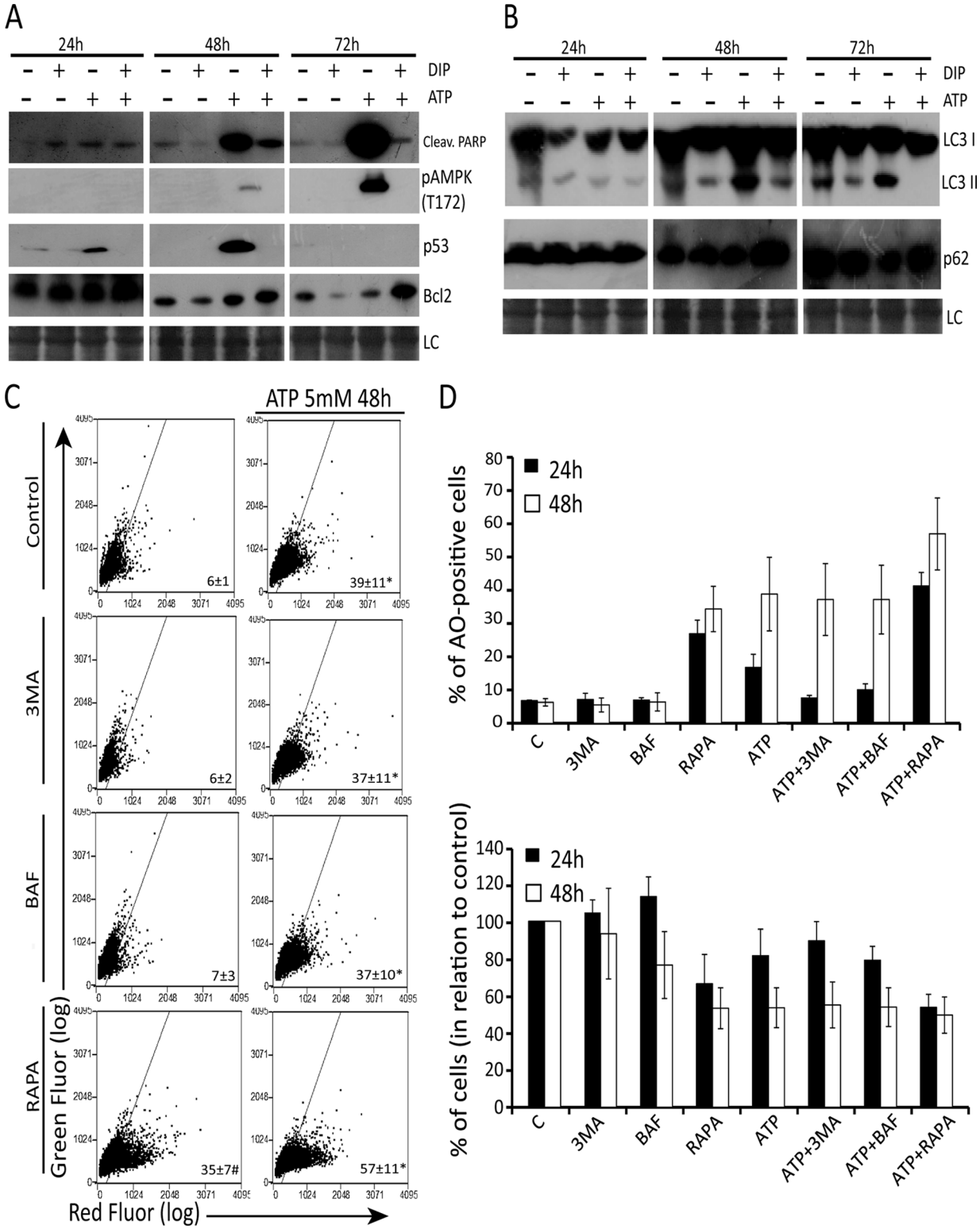

FIGURE 7: Adenosine uptake triggers AMPK phosphoactivation, p53 increase, and cytotoxic autophagy in SiHa cells. Expression of (A) p-AMPK, cleaved PARP, p53, and Bcl-2 and (B) p62 and LC3 II after 5 mM ATP exposure for 24, 48, and 72 h with or without 10 μM DIP pretreatment, determined by Western blot analysis as described in *Materials and Methods*. (C) Effect of the class III autophagy inhibitors 3MA and BAF and autophagy stimulator RAPA on AO staining after 48 h of ATP exposure. SiHa cells were pretreated with 2 mM 3MA, 100 nM BAF, or 200 nM RAPA before ATP treatment, and autophagy index was determined by AO staining as described in *Materials and Methods*. (D) Top, percentage of AO-positive cells after ATP exposure before or not to autophagy inhibitors or stimulator. Bottom, number of viable cells after treatment. Note that treatments that increased autophagy induced a reduction in cell number (see also Supplemental Figure S4). *p <0.05 compared with treatments without ATP; $^{\#}p < 0.05$ compared with control (two-way ANOVA, followed by Bonferroni posttest).

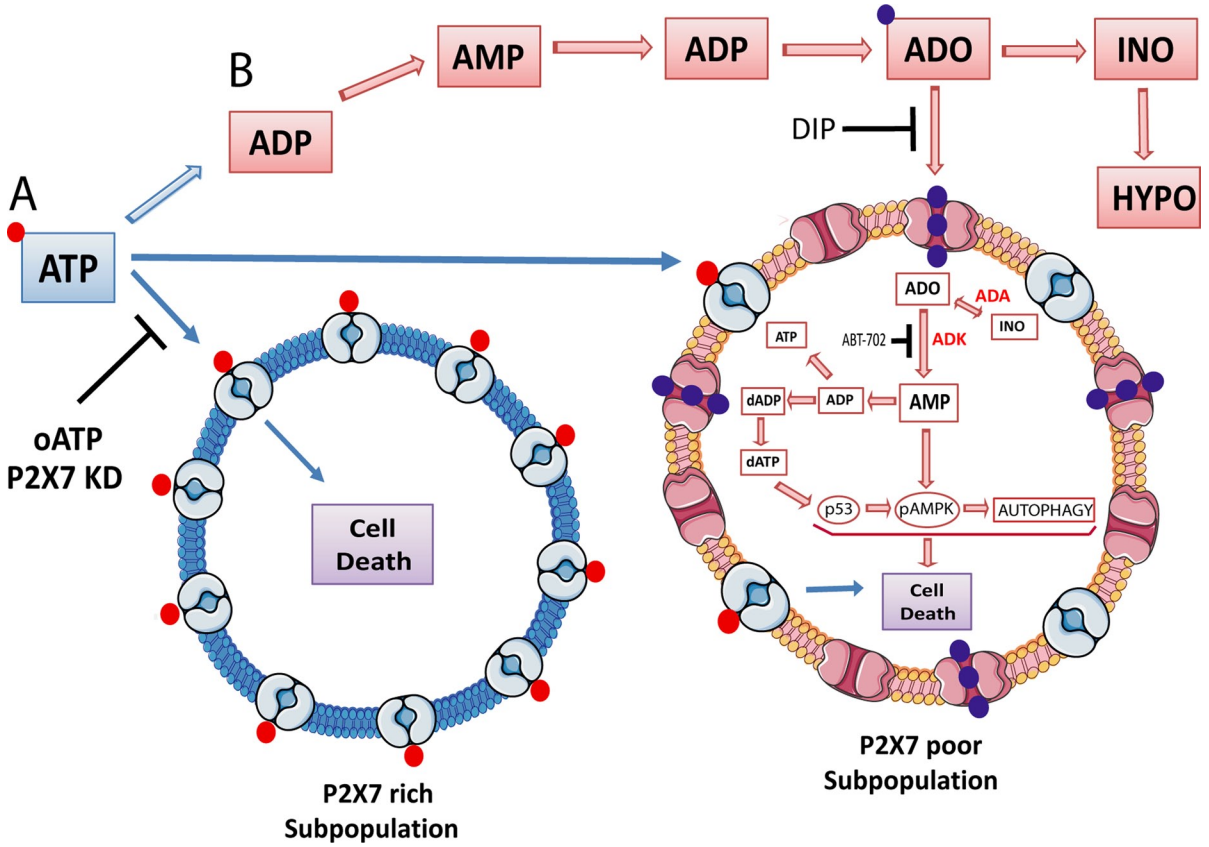

FIGURE 8: Schematic illustration of how adenosine uptake induces SiHa cervical tumor cell death in response to high levels of extracellular ATP. (A) A small subpopulation that expresses high levels of P2×7 died after being exposed to high levels of extracellular ATP via P2×7 activation by an unknown intracellular mechanism. The P2×7 antagonist oATP and receptor knockdown partially blocked ATP-induced cell death. (B) A major subpopulation of cells that express low levels of P2×7 died after being exposed to ATP metabolites such as ADP, AMP, adenosine, inosine, and hypoxanthine. In these cells, adenosine is taken up and partially converted to inosine through adenosine deaminase (ADA) activity. Concomitantly, adenosine is also phosphorylated to AMP by adenosine kinase (ADK), which leads to dATP accumulation, AMPK phosphorylation, p53 activation, autophagy induction, and finally cell death through apoptosis. Dipyridamole (DIP), an adenosine transporter inhibitor, and ABT-702, an adenosine kinase inhibitor, completely blocked cell death induction by these pathways. →, stimulation; –|, inhibition. ADO, adenosine; ADP, adenosine 5′-diphosphate; AMP, adenosine 5′-monophosphate; ATP, adenosine 5′-triphosphate; dADP, deoxyadenosine 5′-diphosphate; dATP, deoxyadenosine 5 -triphospate; HYPO, hypoxanthine; INO, inosine.

was withdrawn, transferred to a microtube on ice, and centrifuged for 1 min at 10,000 rpm, an aliquot of the supernatant was used for enzymatic assay using an LDH kit from Labtest Diagnostica (Minas Gerais, Brazil). Results are expressed as percentage of 0.5% Triton X-100–induced LDH release.

Annexin V and propidium iodide staining

Phosphatidylserine externalization was determined by the annexin fluorescence signal of an annexin V–fluorescein isothiocyanate conjugate (Santa Cruz Biotechnology, Inc, Santa Cruz, CA) according to the manufacturer's protocol. Cell cultures were treated, trypsinized, and centrifuged for 6 min at 1600 rpm, and the supernatant was discarded. The pellet was suspended with 150 µl of annexin binding buffer (10 mM 4-(2-hydroxyethyl)-1-piperazineethanesulfonic acid, pH 7.4, 140 mM NaCl, 2.5 mM $CaCl_2$), incubated with annexin V at 0.75 µl/sample and PI at 15 µl/sample for 15 min at room temperature in the dark, and analyzed on a Guava EasyCyte flow cytometer, using Guava EasyCyte software for analysis (Millipore, Billerica, MA). Cisplatin, 40 µM, was used as positive control for apoptosis, and 0.5% Triton X-100 was used as a positive control for necrosis.

Analysis of intracellular and extracellular ATP metabolism by high-performance liquid chromatography

For extracellular ATP metabolism analysis, SiHa cells (20,000 cells/well) were seeded on 24-well multiwell plates and treated with 5 mM ATP for 24, 48, and 72 h after or not with10 µM DIP pretreatment. After the incubation time, the reaction medium was withdrawn and transferred to a microtube on ice, followed by centrifugation for 1 min at 10,000 rpm, supernatant dilution, and high-performance liquid chromatography (HPLC) analysis. The results are expressed as total amount of the different compounds (nanomoles), represented by the exogenous (added and extracellularly metabolized) plus endogenous (secreted) purinergic compounds, in the respective incubation time. The control for cellular purine secretion was done by growing cells in complete medium (DMEM plus 10% FBS) for 24, 48, and 72 h; very low levels of purinergic compounds were found in the extracellular medium (Supplemental Table S1).

For analysis of intracellular nucleoside triphosphate levels, SiHa cells (96,000 cells/well) were seeded on six-well multiwell plates and treated as described. All extraction steps were performed on ice, as described by Huang *et al.* (2003). The resulting supernatant was stored at –80°C until HPLC analyses. The intracellular concentration

of each nucleotide was normalized by the number of viable cells in the sample and is expressed as nanomoles/10^6 cells.

For HPLC analysis, 40-µl aliquots were applied to a reversed-phase HPLC system (Shimadzu, Japan) using a 15-cm C_{18} Resteck column at 260 nm with a mobile phase containing 60 mM KH_2PO_4 (Sigma-Aldrich) and 5 mM tetrabutylammonium chloride (Sigma-Aldrich), pH 6.0, in 30% methanol according to a previously described method (Casali *et al.*, 2003). All peaks were identified by retention time and comparison with standards. All incubations were carried out in triplicate, and controls to correct for nonenzymatic hydrolysis of nucleotides were done by measuring the peaks present in the same reaction medium incubated without cells.

Pharmacological profile assays

To test whether ATP-induced cell death involves P2×7 activation, we evaluated the effect of agonists and antagonists of this receptor. We seeded SiHa cells (20,000 cells/well) on 24-well multiwell plates and treated them as indicated. For the BzATP dose–response curve, we treated SiHa cells with 50, 100, 150, and 300 mM BzATP for 24 h. The effect of adenosine 5′-*O*-(3 thiotriphosphate) (ATPγS), a nonhydrolyzed P2 agonist, was determined by treating cells with 300 µM ATPγS for 24 h. For blockage of ATP-induced cell death, cells were previously treated with 300 and 600 mM oATP, a nonspecific P2×7 antagonist, for 2 h. After this time of incubation, cells were treated with 5 mM ATP for 24 h. At the end of all treatments, the viable cells were counted as described.

To test whether ATP was degraded and extracellular adenosine uptake was responsible for apoptosis induction, SiHa cells were pretreated with 10 µM DIP for 30 min before addition of 5 mM ATP for 24, 48, and 72 h. At the end of treatment, the viable cells were counted, and apoptosis status was determined by annexin V/IP staining as described. In addition, we investigated the effect of adenosine kinase inhibition on the induction of apoptosis. For this, SiHa cells were pretreated with 100 nM 4-amino-5-(3-bromophenyl)-7-(6-morpholino-pyridin-3-yl)pyrido[2,3-d]pyrimidine (ABT-702), a cell-permeable, adenosine-competitive and reversible adenosine kinase inhibitor, for 30 min, followed by the addition of 5 mM ATP for 48 and 72 h. ABT-702 was replaced every 24 h, and the number of viable cells and apoptosis status were determined after 48 and 72 h as described.

To verify that the mechanism that triggered apoptosis in SiHa cells after ATP exposure was P2×7 pore formation followed by increase of intracellular free calcium ions and caspase activation, we exposed subconfluent cultures to 0.6 mM EGTA, a calcium-chelating agent, or 50 µM zAsp, a pancaspase inhibitor, for 30 min. Then we treated cells with 5 mM ATP for 48 h, 100 µM BzATP for 24 h, or 300 µM ATPγS for 24 h, followed by cell number determination, phenotype observation, and annexin V/IP assay, as described.

Real-time PCR

Total RNA from SiHa, HeLa, C33A, and HaCaT cell lines was isolated with the RNA Mini Kit (Qiagen, Hilden, Germany) in accordance with the manufacturer's instructions. The cDNA species were synthesized with Super-Script II (Life Technologies, Carlsbad, CA) from 5 µg of total RNA in a total volume of 20 µl with both oligo (dT) primer and random hexamers in accordance with the manufacturer's instructions. SYRB Green I–based real-time PCR was carried out on a MJ Research DNA Engine Opticon Continuous Fluorescence Detection System (MJ Research, Waltham, MA), as described (Zerbini *et al.*, 2003). All PCR mixtures contained PCR buffer (final concentration; 10 mM Tris-HCl, pH 9.0, 50 mM KCl, 2.0 mM $MgCl_2$, and 0.1% Triton X-100), 250 µM deoxy-NTP (Roche Molecular Biochemicals, Penzberg, Upper Bavaria, Germany), 0.5 µM of each PCR primer indicated later, 0.5× SYBR Green I (Molecular Probes, Eugene, OR), 5% DMSO, and 1 U of taq DNA polymerase (Promega, Madison, WI) with 2 µl of cDNA in a 25-µl final volume reaction mix. The samples were loaded onto wells of Low Profile 96-well microplates. After an initial denaturation step for 1 min at 94°C, conditions for cycling were 35 cycles of 30 s at 94°C, 30 s at 56°C, and 1 min at 72°C. The fluorescence signal was measured right after incubation for 5 s at 79°C after the extension step, which eliminates possible primer dimer detection. At the end of the PCR cycles, a melting curve was generated to identify specificity for the PCR product. For each run, serial dilutions of human glyceraldehyde-3-phosphate dehydrogenase (GAPDH) plasmids were used as standards for quantitative measurement of the amount of amplified DNA. In addition, for normalization of each sample, human GAPDH primers were used to measure the amount of GAPDH cDNA. All samples were run in triplicate, and the data are presented as the ratio cDNA/GAPDH. For human GAPDH, the primers used were as follows: sense primer, 5′-CAAAGTTGTCATGGATGACC-3′, and antisense primer, 5′-CCATGGAGAAGGCTGGGG-3′. For P2×7, the primers used were as follows: sense primer, 5′- AAA AGC CGG GGG CCT GCA TC-3′, and antisense primer, 5′-GCA GCT GGG CAG GAT GGC AA-3′. Oligonucleotides were obtained from Invitrogen.

Western blot analysis

Cell cultures were washed twice with cold PBS and homogenized in lysis buffer (4% SDS, 2.1 mM EDTA, and 50 mM Tris). Aliquots were taken for protein determination (Peterson, 1983), and β-mercaptoethanol was added to a final concentration of 5%. Thirty micrograms of protein was separated on 12% SDS–PAGE (Bio-Rad, Hercules, CA) and electrotransferred to polyvinylidene fluoride (PVDF) membranes. Membranes were blocked with 5% M-TTBS (5% milk in Tween-20 in Tris-buffered saline [TTBS]) and further incubated with anti-P2×7 antibody (1:500; Santa Cruz Biotechnology), anti-Bcl2 (1:1000), anti-pAMPK (1:1000), anti–cleaved PARP (1:1000), anti-p62 (1:1000), anti-p53 (1:1000), and anti-LC3II (1:1000; Cell Signaling, Danvers, MA), diluted in TTBS, at room temperature. The membranes were then incubated with horseradish peroxidase–conjugated secondary antibody (1:2000) for 2 h at room temperature, and chemiluminescence was detected using x-ray films (X-Omat; Kodak, Rochester, NY). The films were scanned, and the percentage of band intensity was analyzed using ImageJ (National Institutes of Health, Bethesda, MD).

P2×7 knockdown

Human P2RX7 (GeneID 18439) was knocked down by transduction of SiHa cells with lentivirus produced with the plasmid clone ID NM_002562.4-801s1c1 from the Mission RNAi library from Sigma-Aldrich. Nontarget (SHC001) sequence was used as a control. Lentiviruses were produced by cotransfecting the Mission RNAi plasmid with the helper plasmids pRSVREV, pVSV-G, and pMDLgRRE (Dull *et al.*, 1998) in subconfluent Hek293T cells with Superfect Reagent (Qiagen), according to the manufacture's protocol. Three days after transfection, supernatant was collected twice every day for 1 wk, filtered through a 0.22-mm membrane, and used immediately or stored at –80°C. We added 1 ml of virus-containing medium to target cells, also at subconfluent stage (12,000 cells/well) in 24-well plates, together with 8 µg/ml Polybrene overnight. Cells were allowed 48 h to express the selection marker and were then selected with 3 µg/ml puromycin for at least 10 d. Knockdown was confirmed by Western blotting.

Quantification of acidic vacuolar organelles by AO staining

The fluorescent dye AO is a marker of AVOs (acidic vacuolar organelles) that fluoresces green in the whole cell except in acidic compartments (mainly late autophagosomes), where it fluoresces red. AVO formation is a typical feature of autophagy, and its development indicates autophagosomes maturation and an efficient autophagic process, since only mature/late autophagosomes are acidic (Klionsky *et al*., 2008). For AVO determination, cells (20,000 cells/well) were seeded on 24-well multiwell plates and exposed to autophagy inhibitors or inducers. Cells were treated with 2 mM 3MA, a blocker of autophagosome formation, for 1 h; 100 nM BAF, an inhibitor of the late phase of autophagy, for 24 h; or 200 nM RAPA, an autophagy inducer, for 24 h before ATP treatment. After the incubation time, medium was replaced and 5 mM ATP was added for 24 or 48 h. Then cells were trypsinized and incubated with AO (2.7 mM) for 15 min at room temperature, and fluorescence emission was analyzed by flow cytometry, as described previously (Jiang *et al*., 2009), using a Guava flow cytometer and Guava Cytosoft.

Statistical analysis

Statistical analysis was performed with Prism 5 (GraphPad, La Jolla, CA). Data are expressed as percentage of control and presented as mean ± SD of at least three independent experiments. Statistical analyses for comparison among multiple groups were performed by one-way analysis of variance (ANOVA), followed by a Turkey post-hoc test. When more than one molecule was mixed to the same well at the same time, a two-way ANOVA was performed, followed by a Bonferroni posttest. Values were considered significant at $p < 0.05$. Correlation coefficients were calculated using the CORREL function of Excel 2013 (Microsoft, Redmond, WA).

ACKNOWLEDGMENTS

We thank the Brazilian agencies FAPERGS (Fundação de Amparo à Pesquisa do Rio Grande do Sul; Pronem 11/2072-2, Pesquisador Gaúcho 11/0916-1), CNPq (Conselho Nacional de Desenvolvimento Científico e Tecnológico; Universal 472512/2011-0), ICGEB BRA (International Centre for Genetic Engineering and Biotechnology, Brazil; 11/01), CAPES (Coordenação e Aperfeiçoamento de Pessoal de Nível Superior), and PROPESQ (Pró-Reitoria de Pesquisa da Universidade Federal do Rio Grande do Sul) for financial support.

REFERENCES

Baldwin SA, Beal PR, Yao SYM, King AE, Cass CE, Young JD (2004). The equilibrative nucleoside transporter family, SLC29. Pflugers Arch 447, 735–743.

Beckenkamp A, Santana DB, Bruno AN, Calil LN, Casali EA, Paccez JD, Zerbini LF, Lenz G, Wink MR, Buffon A (2014). Ectonucleotidase expression profile and activity in human cervical cancer cell lines. Biochem Cell Biol 92, 95–104.

Bian S, Sun X, Bai A, Zhang C, Li L, Enjyoji K, Junger WG, Robson SC, Wu Y (2013). P2′7 integrates PI3K/AKT and AMPK-RAS40-mTOR signaling pathways to mediate tumor cell death. PLoS One 8, e60184.

Burnstock G, Di Virgilio F (2013). Purinergic signaling and cancer. Purinergic Signal 9, 491–540.

Burnstock G, Knight GE, Greig AVH (2012). Purinergic signaling in healthy and diseased skin. J Invest Dermatol 132, 526–546.

Casali EA, Souza LF, Gelain DP, Kaiser GR, Battastini AM, Sarkis JJ (2003). Changes in ectonucleotidase activities in rat Sertoli cells during sexual maturation. Mol Cell Biochem 247, 111–119.

Di Virgilio F (2012). Purines, purinergic receptors, and cancer. Cancer Res 72, 5441–5447.

Dull T, Zufferey R, Kelly M, Mandel RJ, Nguyen M, Trono D, Naldini L (1998). A third-generation lentivirus vector with a conditional packaging system. J Virol 72, 8463–8471.

Feng L, Sun X, Csizmadia E, Han L, Bian S, Murakami T, Wang X, Robson SC, Wu Y (2011). Vascular CD39/ENTPD1 directly promotes tumor cell growth by scavenging extracellular adenosine triphosphate. Neoplasia 13, 206–216.

Franken NAP, Rodermond HM, Stap J, Haveman J, Van Bree C (2006). Clonogenic assay of cells in vitro. Nat Protoc 1, 2315–2319.

Ghiringhelli F, Bruchard M, Chalmin F, Rébé C (2012). Production of adenosine by ectonucleotidases: a key factor in tumor immunoescape. J Biomed Biotechnol 2012, 473712.

Hardie DG, Hawley SA, Scott JW (2006). AMP-activated protein kinase-development of the energy sensor concept. J Physiol 574, 7–15.

He C, Klionsky DJ (2009). Regulation mechanisms and signaling pathways of autophagy. Annu Rev Genet 43, 67–93.

Huang D, Zhang Y, Chen X (2003). Analysis of intracellular nucleoside triphosphate levels in normal and tumor cell lines by high-performance liquid chromatography. J Chromatrogr B Analyt Technol Biomed Life Sci 784, 101–109.

Jemal A, Bray F, Center MM, Ferlay J, Ward E, Forman D (2011). Global cancer statistics. CA Cancer J Clin 61, 69–90 [correction published in CA Cancer J Clin (2011). 61, 134].

Jiang H, White EJ, Conrad C, Gomez-Manzano C, Fueyo J (2009). Autophagy pathways in glioblastoma. Methods Enzymol 453, 273–286.

Joachims ML, Marble P, Knott-Craig C, Pastuszko P, Blackburn MR, Thompson LF (2008). Inhibition of deoxynucleoside kinases in human thymocytes prevents dATP accumulation and induction of apoptosis. Nucleosides Nucleotides Nucleic Acids 27, 816–820.

Johnston JB (2011). Mechanism of action of pentostatin and cladribine in hairy cell leukemia. Leuk Lymphoma 52(Suppl 2), 43–45.

Kabeya Y, Mizushima N, Yamamoto A, Oshitani-Okamoto S, Ohsumi Y, Yoshimori T (2004). LC3, GABARAP and GATE16 localize to autophagosomal membrane depending on form-II formation. J Cell Sci 117, 2805–2812.

Klionsky DJ, Abeliovich H, Agostinis P, Agrawal DK, Aliev G, Askew DS, Baba M, Baehrecke EH, Bahr BA, Ballabio A, *et al.* (2008). Guidelines for the use and interpretation of assays for monitoring autophagy in higher eukaryotes. Autophagy 4, 151–175.

Kloor D, Yao K, Delabar U, Osswald H (2000). Simple and sensitive binding assay for measurement of adenosine using reduced *S*-adenosylhomocysteine hydrolase. Clin Chem 46, 537–542.

Lee SG, Choi J K, Choi BH, Lim Y, Kim YH, Lee KH, Shin JC, Ahn WS (2006). The effect of adenosine 5-triphosphate on calcium mobilization and cell proliferation in cervical cancer cells. Eur J Obstet Gynecol Reprod Biol 127, 110–114.

Li X, Qi X, Zhou L, Fu W, Abdul-Karim FW, MacLennan G, Gorodeski GI (2009). P2′7 receptor expression is decreased in epithelial cancer cells of ectodermal, uro-genital sinus, and distal paramesonephric duct origin. Purinergic Signal 5, 351–368.

Ma RQ, Yang H, Zhao XH, Zhang YK, Yao AH, Cheng P, Xie YB, Zhao HK, Ju G, Kuang F (2011). The protective effects of inosine against chemical hypoxia on cultured rat oligodendrocytes. Cell Mol Neurobiol 31, 1171–1186.

Matsumoto G, Wada K, Okuno M, Kurosawa M, Nukina N (2011). Serine 403 phosphorylation of p62/SQSTM1 regulates selective autophagic clearance of ubiquitinated proteins. Mol Cell 44, 279–289.

Nogi Y, Kanno T, Nakano T, Fujita Y, Tabata C, Fukuoka K, Gotoh A, Nishizaki T (2012). AMP converted from intracellularly transported adenosine upregulates p53 expression to induce malignant pleural mesothelioma cell apoptosis. Cell Physiol Biochem 30, 61–74.

Obajimi O, Melera PW (2008). The depletion of cellular ATP by AG2034 mediates cell death or cytostasis in a hypoxanthine-dependent manner in human prostate cancer cells. Cancer Chemother. Pharmacol 62, 215–226.

Ohta A, Gorelik E, Prasad SJ, Ronchese F, Lukashev D, Wong MK, Huang X, Caldwell S, Liu K, Smith P, *et al.* (2006). A2A adenosine receptor protects tumors from antitumor T cells. Proc Natl Acad Sci USA 103, 13132–13137.

Pankiv S, Clausen TH, Lamark T, Brech A, Bruun JA, Outzen H, Øvervatn A, Bjørkøy G, Johansen T (2007). p62/SQSTM1 binds directly to Atg8/LC3 to facilitate degradation of ubiquitinated protein aggregates by autophagy. J Biol Chem 282, 24131–24145.

Pellegatti P, Raffaghello L, Bianchi G, Piccardi F, Pistoia V, Di Virgilio F (2008). Increased level of extracellular ATP at tumor sites: in vivo imaging with plasma membrane luciferase. PLoS One 3, e2599.

Peterson GL (1983). Determination of total protein. Methods Enzymol 91, 95–119.

Saitoh M, Nagai K, Nakagawa K, Yamamura T, Yamamoto S, Nishizaki T (2004). Adenosine induces apoptosis in the human gastric cancer cells

via an intrinsic pathway relevant to activation of AMP-activated protein kinase. Biochem Pharmacol 67, 2005–2011.
Sai K, Yang D, Yamamoto H, Fujikawa H, Yamamoto S, Nagata T, Saito M, Yamamura T, Nishizaki T (2006). A1 adenosine receptor signal and AMPK involving caspase-9/-3 activation are responsible for adenosine-induced RCR-1 astrocytoma cell death. Neurotoxicology 27, 458–467.
Schiffman M, Wentzensen N, Wacholder S, Kinney W, Gage JC, Castle PE (2011). Human papillomavirus testing in the prevention of cervical cancer. J Natl Cancer Inst 103, 368–383.
Tamajusuku ASK, Villodre ES, Paulus R, Coutinho-Silva R, Battasstini AMO, Wink MR, Lenz G (2010). Characterization of ATP-induced cell death in the GL261 mouse glioma. J Cell Biochem 109, 983–991.
Tsuchiya A, Kanno T, Saito M, Miyoshi Y, Gotoh A, Nakano T, Nishizaki T (2012). Intracellularly transported adenosine induces MCF-7 human breast cancer cells by accumulating AMID in the nucleus. Cancer Lett 321, 65–72.
Wang Q, Wang L, Feng YH, Li X, Zeng R, Gorodeski GI (2004). P2′7 receptor-mediated apoptosis of human cervical epithelial cells. Am J Physiol Cell Physiol 287, 1349–1358.
Wen LT, Knowles AF (2003). Extracellular ATP and adenosine induce cell apoptosis of human hepatoma Li-7A cells via the A3 adenosine receptor. Br J Pharmacol 140, 1009–1018.
Yang Z, Klionsky DJ (2010). Mammalian autophagy: core molecular machinery and signaling regulation. Curr Opin Cell Biol 22, 2124–131.
Zerbini LF, Wang Y, Cho JY, Libermann TA (2003). Constitutive activation of nuclear factor _B p50/p65 and Fra-1 and JunD is essential for deregulated interleukin 6 expression in prostate cancer. Cancer Res 63, 2206–2215.